Edelweiss Applied Science and Technology
ISSN: 2576-8484
Vol. 9, No. 8, 989-1001
2025
Publisher: Learning Gate
DOI: 10.55214/2576-8484.v9i8.9523
© 2025 by the authors; licensee Learning Gate

Dynamical characterization of rainfall structure and induced-attenuation over coastal regions of south Africa for earth-space links applications

Elijah Olusayo Olurotimi[1*], Kingsley Ogudo[2], Akintunde Alonge[3]
[1,2,3]Department of Electrical and Electronic Engineering Technology, University of Johannesburg, South Africa; elisayrot@gmail.com (E.O.O.).

Abstract: Rainfall structure characterization and the corresponding induced attenuation are crucial for accurately predicting signal outages in Earth-space propagation links, hydrology, and meteorology. This paper analyzes five years of data on 60-minute integrated rainfall collected from the South African Weather Service across three coastal locations in the Republic of South Africa, with applications in radio wave communication. The study employs recommendations from the International Telecommunication Union Radiocommunication Sector to convert higher 60-minute integration data to 1-minute intervals and to determine the rain height necessary for predicting rain-induced attenuation in Earth-space links. The results confirm that oceanic currents influence rainfall structure at these locations. The derived 1-minute rainfall rates correspond to different percentages of time, including the lower percentage of 0.01% for internet access and the even lower percentage of 0.001% required for multimedia applications. The 0.01% time percentage was used to verify rain-induced attenuation at higher frequency bands, emphasizing the importance of precise rainfall characterization for reliable communication system design and meteorological analysis.

Keywords: *Coastal regions X, Integration time, Rainfall attenuation, Rainfall structure.*

1. Introduction

The growing proliferation of communication networks has created congestion in lower frequency bands, leading system designers to investigate higher frequencie [1-10]. Rainfall is the most common source of attenuation at higher frequencies, especially in tropical and subtropical locations, and it can considerably affect system performance [1, 11-16]. Understanding rainfall parameters and their impact on microwave signal attenuation is critical for maximizing system capacity while meeting quality and reliability standards [1]. High-resolution and accurate rainfall rate information from several sites is critical in designing and evaluating the microwave systems (both terrestrial and satellite). The rainfall rate is the primary parameter that attenuates microwave signals and significantly impacts the telecommunications services delivered [17-21].

As a result, understanding rainfall structure and attenuation over any location of interest is critical for adequately planning reliable microwave communication systems. Rain attenuation predictions require a 1-minute integration of rainfall rate data. This 1-minute rainfall is also necessary for various other activities and applications, including space vehicles, aerospace, and radar systems [22-24]. In observing the 1-minute rainfall rate, the combination of rainfall structure and attenuation characteristics is critical because of the variability in the advancing pattern of digital interactions via communication satellites functioning at higher frequencies [17]. However, the rainfall rate and attenuation data necessary at specific sites are limited, necessitating the development of models to estimate the location dependence of rainfall rate and attenuation.

This study evaluates rainfall structure and attenuation across three South African coastal cities using the South African Weather Service's 5-year (2016-2020) 60-minute integrated rainfall data [25].

© 2025 by the authors; licensee Learning Gate
History: Received: 13 June 2025; Revised: 1 August 2025; Accepted: 4 August 2025; Published: 19 August 2025
* Correspondence: elisayrot@gmail.com

Numerous studies have been conducted on rainfall-related topics, such as generating a conversion factor using rain sizing at a specific place [26], developing rainfall rate contour maps from 5 minutes to 1 minute [27], and developing rain attenuation contour maps throughout South Africa [28]. However, the rainfall structure has not been defined across the country, necessitating the need for this study.

The remaining sections of the paper discussed South Africa's coastal climates, the source of the data, and the methods used in the work, where International Telecommunication Union-Radiocommunication (ITU-R) models were extensively used in converting higher integration times of the rainfall data to 1-minute as required for accurate rain attenuation for terrestrial and Earth-space satellite links. This work focuses solely on rain attenuation of Earth-space links, and the methods are presented. The findings were also given, and we concluded the work.

2. South African Coastal Climate, Data Source and Methods

In these sections, we discussed the climates of the selected locations, source of data, and methods.

2.1. South African Coastal Climate

The Republic of South Africa's coastal climate has a unique climatic characteristic that has far-reaching consequences for the economy, the environment, and population well-being. It moves along the southern hemisphere's coastline and is influenced by the chilly Benguela and warm Agulhas Currents, which flow west and east. It can also be separated into three coasts: west, south, and east. South Africa, a subtropical country, receives yearly precipitation, primarily rainfall. This fluctuating climate uniqueness is the primary subject of this research, particularly satellite propagation studies.

Durban, Gqeberha, and Cape Town were chosen as the three locations because of their vibrant, appealing, and heavily populated traits and their different and diverse climates, which reflect the Republic's general climate. These cities are spread across the Republic's coastline on two different world oceans (the Atlantic and the Indian), each with its distinct climate. Furthermore, each year, the cities draw millions of travellers and consumers who use satellite communications to access services. Durban, one of the province's major cities (KwaZulu-Natal), is noted for its magnificent beaches and rich cultural heritage. It is on the Republic's east coast, near the Indian Ocean. Summers in the city are typically temperate and humid, while winters are warm. Gqeberha is the Eastern Cape province's largest city and main seaport. It is situated on the Republic's southern coast, near the western part of Algoa Bay. The city enjoys a warm, oceanic climate. Cape Town is well known for its historical significance and status as the legislative capital. It is situated on the Republic's southern coast, between the Atlantic Ocean and the renowned Table Mountain, and has wet winters and dry summers. Table 1 provides more information on the study's location.

Table 1.
Geographical features of the selected coastal locations.

City	Latitude (°S)	Longitude (°E)	Climatic Region	Altitude(m)	Elevation Angle(°)
Durban	29° 97'	30° 95'	Coastal Savannah	8	38.4
Gqeberha	33° 57'	25° 36'	Oceanic	60	33.3
Cape Town	33° 58'	18° 36'	Mediterranean	42	26.4

2.2. Data Source

This investigation relied on the South African Weather Service (SAWS) data. The National Meteorological Service, Republic of South Africa [25], is a government agency that provides important weather information such as weather reports, climate monitoring, alerts and forecasts. The consistency and reliability of SAWS data is a critical condition for using the agency's meteorological data. This reliance on SAWS data connects us to a more extensive network of researchers who rely on its accuracy. SAWS measures meteorological features using automated weather stations (AWS) equipped with a

Edelweiss Applied Science and Technology
ISSN: 2576-8484
Vol. 9, No. 8: 989-1001, 2025
DOI: 10.55214/2576-8484.v9i8.9523
© 2025 by the authors; licensee Learning Gate

range of electronic sensors, such as tipping bucket rain gauges for measuring rainfall and have been validated based on different metric measures [29, 30]. The AWS automatically records meteorological information and sends it at regular 60-minute integration intervals, guaranteeing that the rainfall data utilized in our study is valid for five years (2016-2020).

2.3. Overview of ITU-R Recommendations

The ITU-R recommendations are internationally recognized standards for radiocommunication systems developed by the International Telecommunication Union's (ITU) Radiocommunication sector, which oversees the international radio-frequency spectrum, geostationary satellites, and developing global radiocommunication standards. They discussed system characteristics, measurements, methodologies, and other technical information relevant to the operation and development of radiocommunication systems. Each piece of advice includes one or more methods for reaching a specific goal, and radiowave propagation is crucial. This work employs a variety of long-range radiowave propagation rules, which are the models necessary when no local model has been developed. The models are as follows.

2.3.1. Recommendation 837-7 (ITU-R Rec. P. 837-7)

This recommendation is the model that caters for the conversion of rainfall rate distribution from higher time to 1-minute integration time which is required in determining accurate rain attenuation. It falls within the category of empirical models known as Global ITU-R Rec. P.837-7 [31]. The model depends on the connection between the equiprobable rainfall rates estimated from an integration time of T and of 1-minute, respectively, and expressed as:

$$R_1(P) = a(T)R_T(P)^{b(T)} \quad (1)$$

where $R_1(P)$and $R_T(P)$ are the dependent integration times, while P is the common probability level, with coefficients $a(T)$and $b(T)$ as provided by [32], as the average obtained by power law regression over a multiple database measurements from different regional climatic countries [33].

2.3.2. Recommendation 839-4 (ITU-R Rec. P. 839-4)

Rain height, h_R, is one of the important parameters to determine rain attenuation. The ITU-R recommended this technique and developed it in connection to the 0° C isotherm level by ITU-R P.839-4. It is provided for many climate locations across the world when there is no specific or restricted information. This section only considers the technique linked to the Southern Hemisphere climate. The h_R can be estimated by the mean 0° C isotherm height, h_o, represented in equation (2) and (3) both in km [34, 35]:

$$h_o = 5 + 0.1(\varphi + 21) \quad \text{for } -71 \leq \varphi < -21 \quad (2)$$

$$h_R = h_o + 0.36 \quad (3)$$

where φ is the latitude in degrees.

2.3.3. Recommendation 618-11 (ITU-R Rec. P. 618-11)

This work employed a long-term statistical method to estimate slant-path rain attenuation at a specified location for frequencies up to 55 GHz, as suggested by [36]. Figure 1 presents the schematic of the Earth-space path and its parameters. The steps required are as follows:

Edelweiss Applied Science and Technology
ISSN: 2576-8484
Vol. 9, No. 8: 989-1001, 2025
DOI: 10.55214/2576-8484.v9i8.9523
© 2025 by the authors; licensee Learning Gate

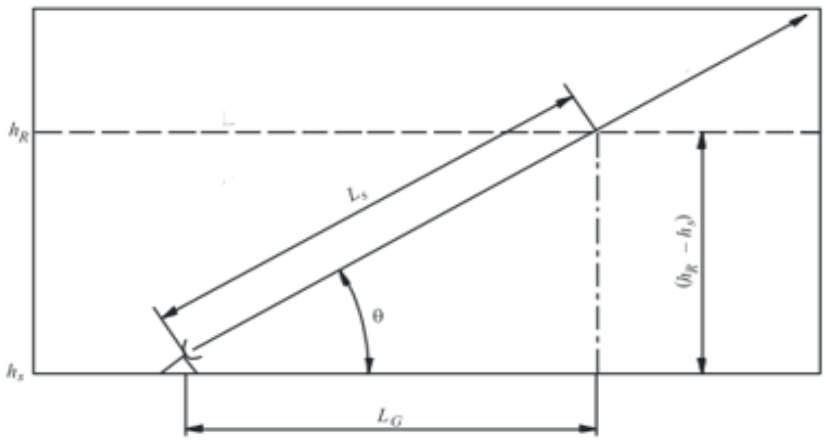

Figure 1.
The Earth-space path [36].

Step 1: Evaluation of h_R, using (3); determination of slant-path, L_s for $\theta \geq 5°$ along with its horizontal projection, L_G with the expressions in (3 and 4)

$$L_s = \frac{(h_R - h_s)}{\sin\theta} \quad (4)$$

$$L_G = L_s \cos\theta \quad (5)$$

Step 2: Computation of the rainfall rate exceeded 0.01%, $R_{0.01}$, at 1-minute integration time for an average year from section 2.3.1.

Step 3: Computation of the specific attenuation (dB/km), γ_R, using the frequency-dependent constant coefficients k and α in [37] with $R_{0.01}$ computed in Step, using (6):

$$\gamma_R = k(R_{0.01})^{\alpha} \quad (6)$$

Step 4: Determination of the horizontal reduction and vertical adjustment factors, $r_{0.01}$ and $v_{0.01}$ in (7 and 8) for 0.01% exceedance:

$$r_{0.01} = \frac{1}{1 + 0.78\sqrt{\frac{L_G \gamma_R}{f}} - 0.38(1 - e^{-2L_G})} \quad (7)$$

Step 5: The factor, , computation for 0.01% of the time

$$\zeta = \tan^{-1}\left(\frac{h_R - h_s}{L_G\, r_{0.01}}\right) \quad \text{degrees}$$

For $\zeta > \theta$,

$$L_R = \frac{L_G r_{0.01}}{\cos\theta}$$

Else,

$$L_R = \frac{h_R - h_s}{\sin\theta}$$

If $|\varphi| < 36°$, $\chi = 36 - |\varphi|$ degrees

Else, $\chi = 0$ degrees

$$v_{0.01} = \frac{1}{1 + \sqrt{\sin\theta}\left(31\left(1 - e^{-(\theta/(1+\chi))}\right)\sqrt{\frac{L_G \gamma_R}{f^2}} - 0.45\right)} \quad (8)$$

Step 6: The effective path-length is:

$$L_E = L_R v_{0.01} \quad \text{km} \quad (9)$$

Step 7: The attenuation exceeded by 0.01% prediction of an average year can be obtained from:

$$A_{0.01} = \gamma_R L_E \quad \text{dB} \quad (10)$$

Edelweiss Applied Science and Technology
ISSN: 2576-8484
Vol. 9, No. 8: 989-1001, 2025
DOI: 10.55214/2576-8484.v9i8.9523
© 2025 by the authors; licensee Learning Gate

Step 8: The estimation of the attenuation exceeded for the remaining percentages of an average year, ranges from 0.001% to 5%, can be estimated from the expressions in (10):

If $p < 1\%$ and $|\varphi| < 36°$ and $\theta \geq 25°$: $\beta = -0.005(|\varphi| - 36)$

If $p \geq 1\%$ or $|\varphi| \geq 36°$: $\beta = 0$

Otherwise: $\beta = -0.005(|\varphi| - 36) + 1.8 - 4.25 \sin\theta$

$$A_p = A_{0.01}\left(\frac{p}{0.01}\right)^{-(0.655 + 0.033 \ln(p) - 0.045 \ln(A_{0.01}) - \beta(1-p)\sin\theta)} \text{ dB} \quad (11)$$

Also, the parameters attributed to Figure 1 are h_s as the height above mean sea level of the earth station (km); $R_{0.01}$ is the point rainfall rate for the location of interest of an average year (mm/h) at 0.01%; θ is the elevation angle; φ is the latitude of the earth station measures in degrees; and f (GHz) is the frequency. All these parameters are utilized in this work.

3. Results and Discussion

The results of the higher integrated time rainfall measured in 60-minute intervals, its conversion to 1-minute and rain-induced attenuation were discussed in this section.

3.1. Rain Rate Distribution

Coastal locations are characterized as areas with high yearly rainfall. Understanding the rainfall rate over each year is crucial as the selected locations of this study are characterized by the type of oceanic currents experienced over the locations. Table 2 presents the annual accumulated rainfall rate (mm) observed from 2016 to 2020. We generally observed some annual variations across the locations with a particular location trend where the highest rainfall rate was recorded over Durban, followed by Gqeberha and Cape Town, recorded the least with 5-year averages of about 1001.68, 469.12 and 357.26 mm, respectively. It can be observed that Durban recorded its highest in 2016, followed by 2017, 2020, 2019, and 2018, which recorded the lowest. Gqeberha rainfall was different, with the highest recorded in 2020, followed by 2017, 2016, and 2018 and the lowest in 2019. However, Cape Town recorded its variation with the highest in 2018, followed by 2016, 2020, and 2019 and lowest in 2017. The dissimilarities of the rate over the locations may be due to the types of climates, influence of oceanic currents and geographical locations.

Table 2.
Annual accumulated rainfall rate.

	2016	2017	2018	2019	2020	5-yr Average
Durban	1242.6	1093.6	672.4	935.2	1064.6	1001.68
Gqeberha	443.4	495	406.2	402.4	598.6	469.12
Cape Town	385.2	280.8	414	325.4	380.9	357.26

Figure 2 presents the 60-minute yearly cumulative distribution comparing the three study locations. The general observation here is that the rainfall rate in Durban recorded higher values than in other locations. Not all rainfall rates over all locations reached the point rainfall rate $R_{0.01}$ at 0.01% required for rain attenuation stats. For instance, in Figure 2(a), Durban achieves approximately 0.01%, Gqeberha could only attain 0.023%, and Cape Town attains 0.03%. In Figure 2(b, c and f), both Durban and Gqeberha attained 0.01%, while Cape Town attained 0.08%, 0.07% and 0.03%, respectively. Only Gqeberha attained 0.01% in Figure 2(d), while Durban and Cape Town attained 0.02%. Also, Figure 2(e) shows that the three locations attain 0.01%. This indicates the need for a 1-minute rainfall rate to determine the accurate rainfall rate over any location of interest.

Edelweiss Applied Science and Technology
ISSN: 2576-8484
Vol. 9, No. 8: 989-1001, 2025
DOI: 10.55214/2576-8484.v9i8.9523
© 2025 by the authors; licensee Learning Gate

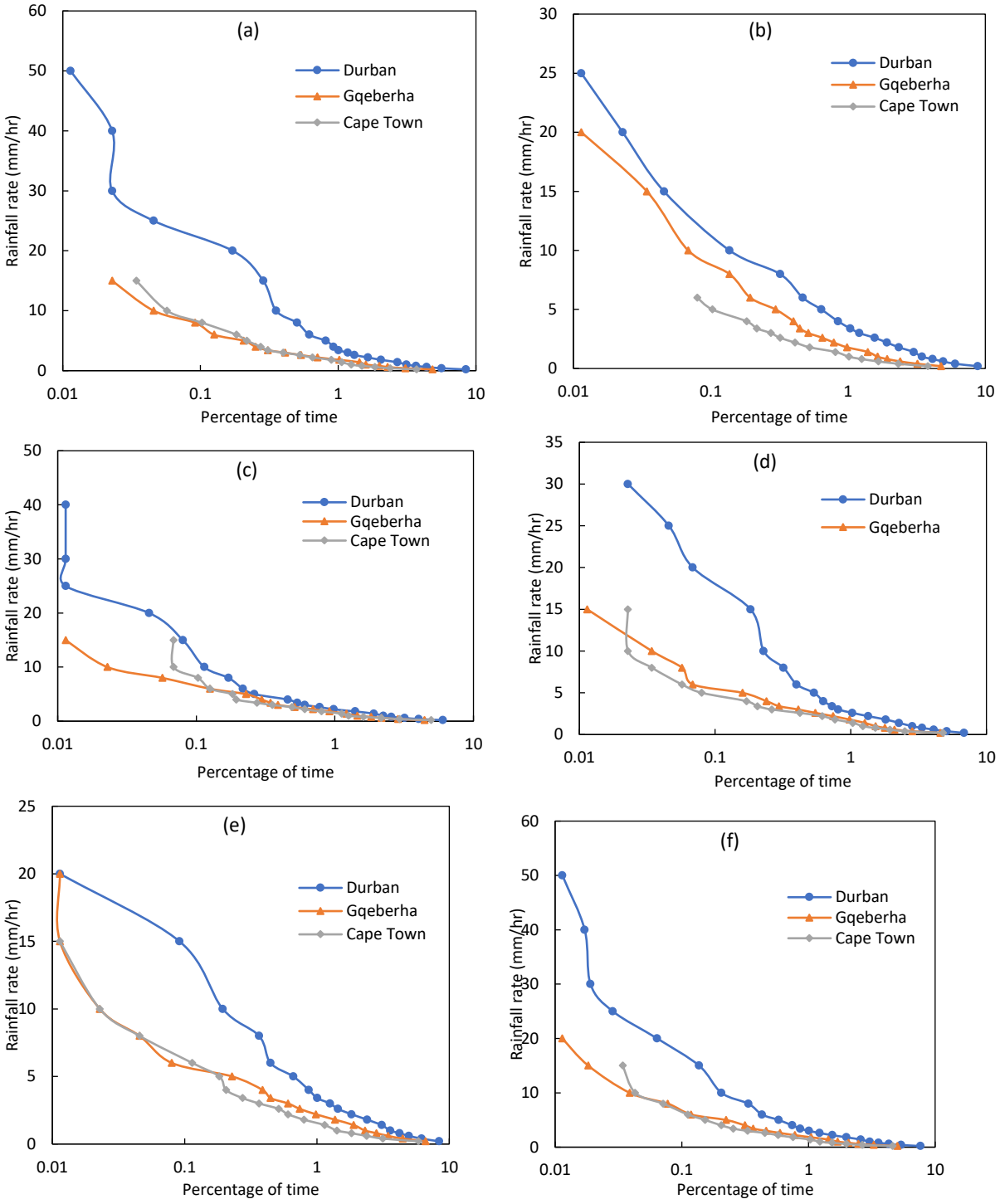

Figure 2.
Annual comparison of 60-minute rainfall rate cumulative distribution over (a) 2016, (b) 2017, (c) 2018, (d) 2019, (e) 2020 and (f) 5-year average.

Edelweiss Applied Science and Technology
ISSN: 2576-8484
Vol. 9, No. 8: 989-1001, 2025
DOI: 10.55214/2576-8484.v9i8.9523
© 2025 by the authors; licensee Learning Gate

3.2. Dynamic Variability of Rainfall Events

Understanding the rainfall rate over a certain threshold is critical for designing radio transmission and satellite systems. Figure 3 depicts the frequency of exceedance and rainfall thresholds at the three sites. Twenty-three thresholds with rainfall rates ranging from 0.2 to 70 mm/h were used. The findings showed that Durban had a higher frequency of rainfall across all thresholds than Gqeberha, while Cape Town had the lowest. Also, the decreasing rainfall rate had a substantial impact on the thresholds. The phenomena in Durban and Cape Town could be related to unique currents influencing rainfall rates in Durban, resulting in increased thresholds. The findings revealed that a higher threshold indicates that the system availability will not meet the required criteria unless an additional buffer is incorporated.

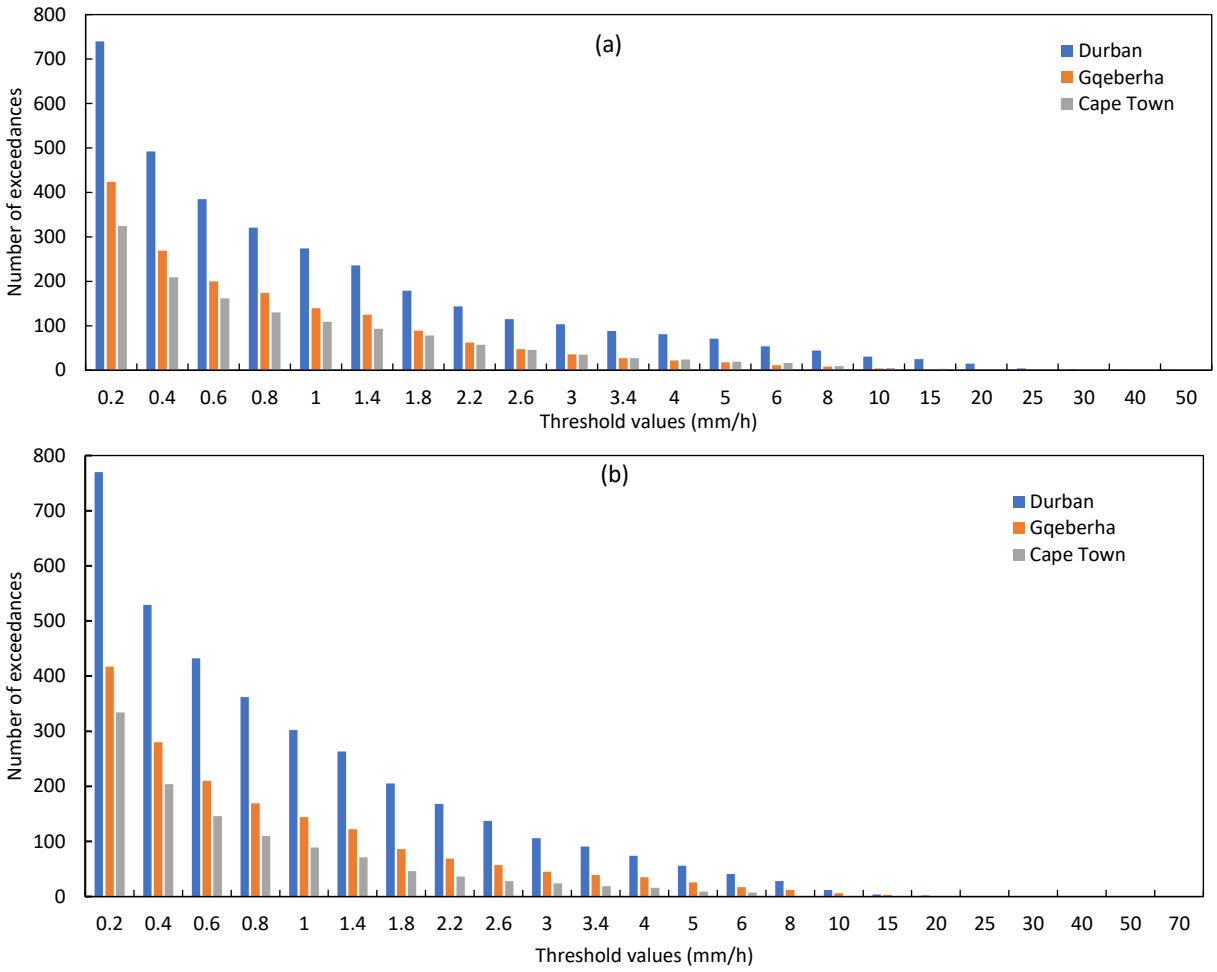

Edelweiss Applied Science and Technology
ISSN: 2576-8484
Vol. 9, No. 8: 989-1001, 2025
DOI: 10.55214/2576-8484.v9i8.9523
© 2025 by the authors; licensee Learning Gate

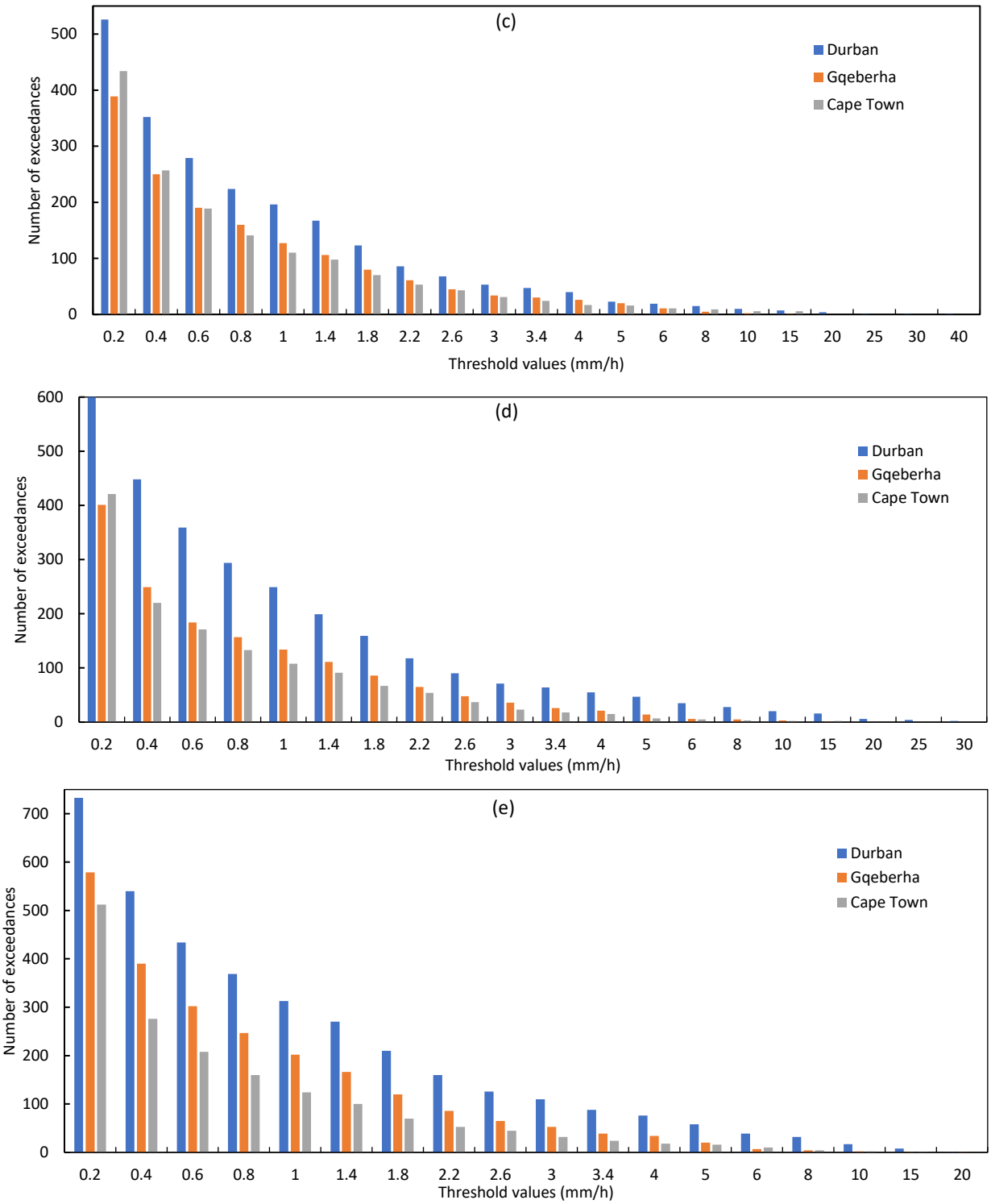

Figure 3.
Thresholds of rainfall rate over (a) 2016, (b) 2017, (c) 2018, (d) 2019, and (e) 2020.

Edelweiss Applied Science and Technology
ISSN: 2576-8484
Vol. 9, No. 8: 989-1001, 2025
DOI: 10.55214/2576-8484.v9i8.9523
© 2025 by the authors; licensee Learning Gate

3.3. Annual Comparison of 1-Minute Cumulative Rainfall Rate Distribution

Figure 4 demonstrates the annual variability of 1-minute rainfall rate distribution over the three locations using the model from section 2.3.1. Most distributions achieved the required lower percentage of time (0.01%), while few attained the lowest percentage 0.001% of time. Also, the trend shows that the lower the rainfall rates, the higher the percentage of time and the higher the rainfall rate, the lower the percentage of time. In Figure 4(a), the highest rainfall rate of about 118.9 mm/h was observed in Durban, while the same rates of about 22.2 m in Gqeberha and Cape Town, although the lowest percentage of times are different, which was about 0.001, 0.003, and 0.005%, respectively. However, at the lower percentage of 0.01%, the rainfall observed is about 45.2, 12.0 and 12.6 m over Durban, Gqeberha and Cape Town, respectively. In Figure 4(b and c), a similar trend was observed as both Durban and Gqeberha attained the lowest and lower percentages (0.001 & 0.01%) while Cape Town attained 0.02% and 0.012%, respectively. Figure 4(d and f) show a similar trend. Only Gqeberha attained the lowest percentage of 0.001%, and Durban and Cape Town exceeded the lower percentage of 0.01%; the values observed at 0.01% are also similar. Figure 4(e) shows the three locations attained the lowest percentage of 0.001% with the rainfall rate at 33.14 mm/h for both Durban and Gqeberha, while in Cape Town, the rainfall rate was 22.19 mm/h; at a lower percentage of time (0.01%), the rainfall rates are 25.0, 7.5 and 8.2 mm/h over Durban, Gqeberha and Cape Town, respectively. This information is crucial in designing high-frequency communication systems over these locations.

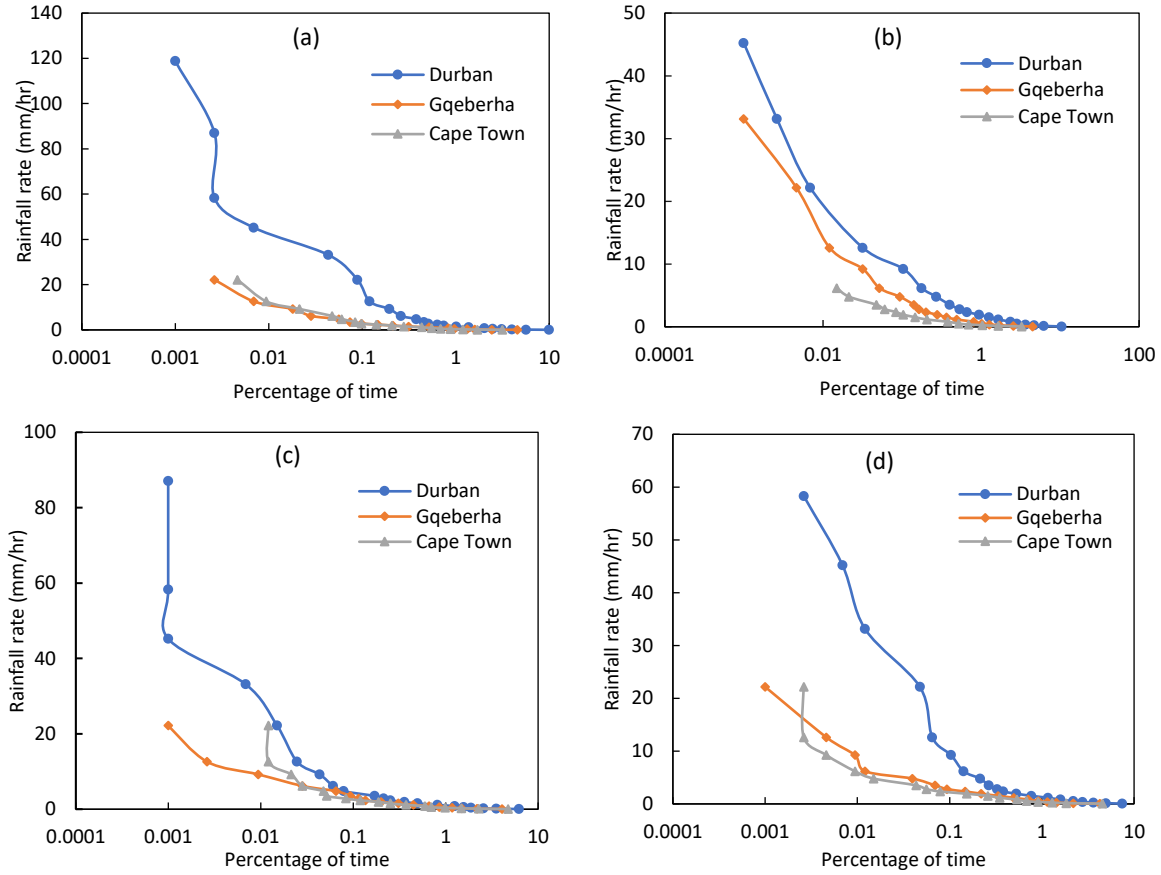

Edelweiss Applied Science and Technology
ISSN: 2576-8484
Vol. 9, No. 8: 989-1001, 2025
DOI: 10.55214/2576-8484.v9i8.9523
© 2025 by the authors; licensee Learning Gate

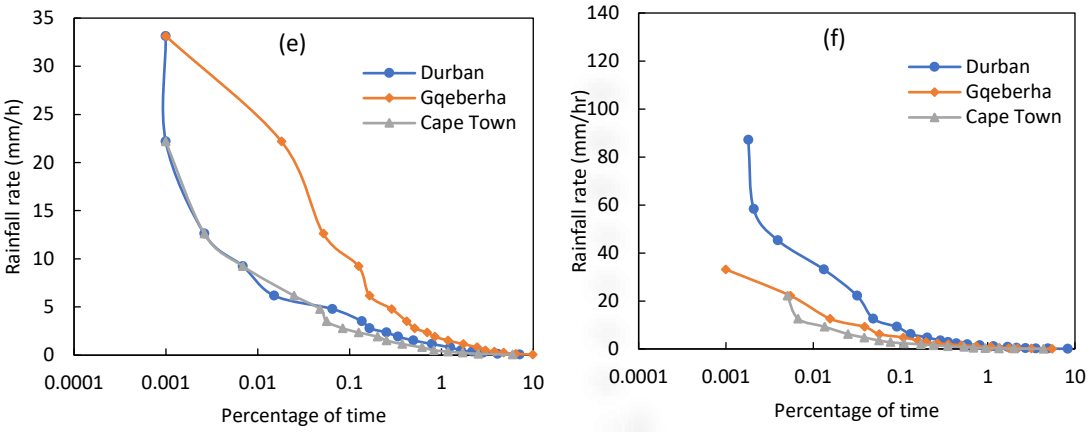

Figure 4.
Annual comparison of 1-minute rainfall rate cumulative distribution over (a) 2016, (b) 2017, (c) 2018, (d) 2019, (e) 2020 and (f) 5-year average.

3.4. Attenuation on Earth-Space Links

Figure 5 presents the cumulative rain-induced attenuation distribution from the point rainfall rate over the study locations using the recommendation in section 2.3.3. It could be observed that the frequencies increase as the attenuation increases, while the rain-induced attenuation decreases in values as the percentage of time increases. In Figure 5(a), the percentages unavailability of 1%, 0.1%, 0.01% and 0.001% of the time at 12 GHz frequency give the attenuation value of about 0.59 dB, 2.55 dB, 7.82 dB and 16.89 dB over Durban, while 0.31, 1.40, 4.55 and 10.39 dB over Gqeberha, then 0.26, 1.23, 4.03 and 9.32 dB over Cape Town, respectively. Also, it produced higher attenuation values at 20 GHz than at 12 GHz, such as percentages of times of 1%, 0.1%, 0.01% and 0.001%; the prediction gives 1.98, 7.75, 21.39 and 41.63 over Durban, while over Gqeberha was 1.06, 4.39, 12.80 and 26.27 dB, then Cape Town gives 0.93, 3.88, 11.42 and 23.73 dB, respectively. However, in Figure 5(b), the rain-induced attenuation values at 1%, 0.1%, 0.01% and 0.001% of times are about 7.12 dB, 24.99 dB, 61.85 dB and 107.83 dB over Durban; 4.06, 14.96, 38.83 and 71.05 over Gqeberha; and 3.61, 13.44, 35.24 and 64.13 dB over Cape Town, respectively at 40 GHz. These statistics are crucial in constructing low-margin Ku and Ka-band systems for communication.

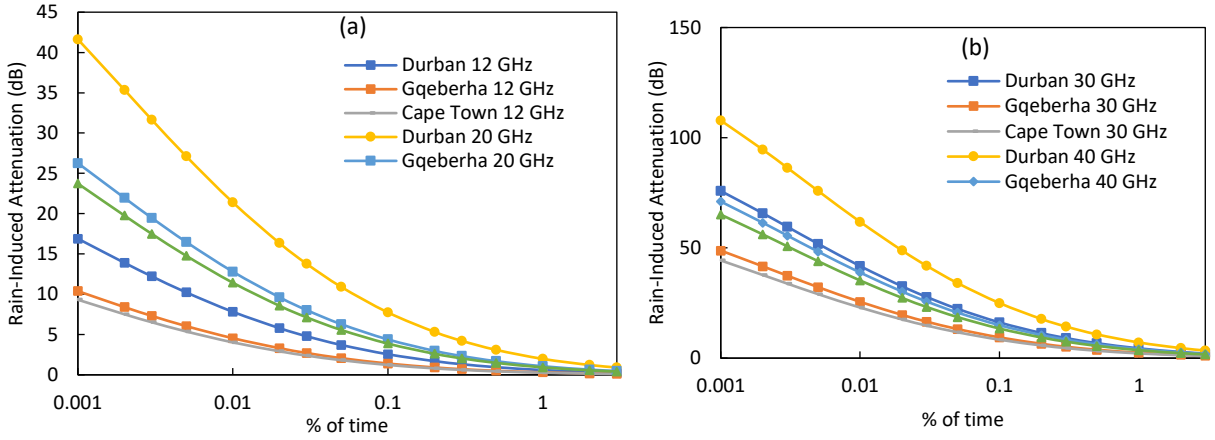

Figure 5.
(a) Ku band and (b) Ka band over the three locations of the study.

Edelweiss Applied Science and Technology
ISSN: 2576-8484
Vol. 9, No. 8: 989-1001, 2025
DOI: 10.55214/2576-8484.v9i8.9523
© 2025 by the authors; licensee Learning Gate

4. Conclusion

This article evaluates rainfall structure and attenuation across three South African coastal areas. The study depicts annual fluctuations in accumulated rainfall rate, measured 60-minute rainfall rate, threshold rainfall observed, 1-minute anticipated integration time, and predicted rain-induced attenuation across three locations. The annual rainfall rate measured demonstrates fluctuations driven by oceanic currents over time, with Durban receiving more rainfall than Gqeberha and Cape Town receiving the least during the study period. Other components of the investigation revealed similar influences on oceanic currents. The findings of this study will be essential for satellite system engineers who are reviewing and constructing microwave transmission communication systems with high data rates and speeds.

Transparency:

The authors confirm that the manuscript is an honest, accurate, and transparent account of the study; that no vital features of the study have been omitted; and that any discrepancies from the study as planned have been explained. This study followed all ethical practices during writing.

Acknowledgment:

The authors would like to that SAWS for providing the data used in this study. The authors also acknowledge the support and express gratitude to the University of Johannesburg's University Research Committee (URC) grant for Prof. KA Ogudo and the Department of Electrical and Electronic Engineering Technology. This work was partly supported by a grant from the University of Johannesburg Library Research Funds (UJ).

Copyright:

© 2025 by the authors. This article is an open access article distributed under the terms and conditions of the Creative Commons Attribution (CC BY) license (https://creativecommons.org/licenses/by/4.0/).

References

[1] M. R. Islam, M. A. Rahman, F. Anwar, and M. M. Rashid, "Performance investigation of earth-to-satellite microwave link due to rain fade in Bangladesh," in *11th International Conference on Computer and Information Technology*, 2008: IEEE, pp. 773-778.

[2] H. Attar *et al.*, "A Review of 6G Conceptual Components, Its Ultra-Dense Networks, and Research Challenges towards Cyber-Physical-Social Systems," *International Journal of Crowd Science*, 2024.

[3] H. Muzammal *et al.*, "Climate Change Impacts on Water Resources and Implications for Agricultural Management," in *Transforming Agricultural Management for a Sustainable Future: Climate Change and Machine Learning Perspectives*: Springer, 2024, pp. 21-45.

[4] S. Kang *et al.*, "Cellular wireless networks in the upper mid-band," *IEEE Open Journal of the Communications Society*, 2024.

[5] B. Al Homssi *et al.*, "Deep learning forecasting and statistical modeling for Q/V-band LEO satellite channels," *IEEE Transactions on Machine Learning in Communications and Networking*, vol. 1, pp. 78-89, 2023.

[6] H. Attar *et al.*, "5G system overview for ongoing smart applications: Structure, requirements, and specifications," *Computational Intelligence and Neuroscience*, vol. 2022, no. 1, p. 2476841, 2022. https://doi.org/10.1155/2022/2476841

[7] I. F. Akyildiz, C. Han, Z. Hu, S. Nie, and J. M. Jornet, "Terahertz band communication: An old problem revisited and research directions for the next decade," *IEEE Transactions on Communications*, vol. 70, no. 6, pp. 4250-4285, 2022.

[8] E. Khorov, A. Krasilov, M. Susloparov, and L. Kong, "Boosting TCP & QUIC performance in mmWave, terahertz, and lightwave wireless networks: A survey," *IEEE Communications Surveys & Tutorials*, vol. 25, no. 4, pp. 2862-2891, 2023.

[9] D. Serghiou, M. Khalily, T. W. C. Brown, and R. Tafazolli, "Terahertz channel propagation phenomena, measurement techniques and modeling for 6G wireless communication applications: A survey, open challenges and future research directions," *IEEE Communications Surveys & Tutorials*, vol. 24, no. 4, pp. 1957-1996, 2022.

[10] R. Chataut, M. Nankya, and R. Akl, "6G networks and the ai revolution—exploring technologies, applications, and emerging challenges," *Sensors*, vol. 24, no. 6, p. 1888, 2024. https://doi.org/10.3390/s24061888

[11] S. Hossain, "Rain attenuation prediction for terrestrial microwave link in Bangladesh," *arXiv preprint arXiv:1406.5038*, 2014. https://arxiv.org/abs/1406.5038

[12] J. S. Ojo and T. V. Omotosho, "Comparison of 1-min rain rate derived from TRMM satellite data and raingauge data for microwave applications in Nigeria," *Journal of Atmospheric and Solar-Terrestrial Physics*, vol. 102, pp. 17-25, 2013.

[13] A. I. O. Yussuff, I. E. Koleoso, and N. H. H. Khamis, "Investigating rain attenuation models for satellite links in tropical Nigeria," *Indonesian Journal of Electrical Engineering and Informatics (IJEEI)*, vol. 6, no. 1, pp. 61-69, 2018. https://doi.org/10.52549/ijeei.v6i1.263

[14] A. S. Bohari, A. I. Abdullah, A. F. Ismail, and K. Badron, "Conversion of 15-Minutes to 1-Minute Rainfall Distribution Derived from Tropical Rainfall Distribution Measurement," in *Journal of Physics: Conference Series*, 2022, vol. 2312, no. 1: IOP Publishing, p. 012085.

[15] E. Alozie *et al.*, "A review on rain signal attenuation modeling, analysis and validation techniques: Advances, challenges and future direction," *Sustainability*, vol. 14, no. 18, p. 11744, 2022.

[16] M. Yusof, N. Najwa, and L. H. Yin, "Enhancing millimeter-wave communication: a tropical perspective on raindrop size distribution and signal attenuation," *International Journal of Electrical & Computer Engineering (2088-8708)*, vol. 15, no. 1, 2025.

[17] J. S. Ojo, M. O. Ajewole, and E. O. Olurotimi, "Characterization of Rainfall Structure and Attenuation Over Two Tropical Stations in Southwestern, Nigeria for the Evaluation of Microwave and Millimeter-Wave Communication Links," *Journal of Meteorology and Climate Science*, vol. 11, no. 1, pp. 40-48, 2013.

[18] C. Ooi Wei and J. Singh Mandeep, "Empirical methods for converting rainfall rate distribution from several higher integration times into a 1-minute integration time in Malaysia," *Geofizika*, Article vol. 30, no. 2, pp. 143-154, 2013. [Online]. Available: https://search.ebscohost.com/login.aspx?direct=true&AuthType=shib&db=a9h&AN=94335476&site=eds-live&scope=site&custid=s5210036

[19] E. O. Olurotimi and K. A. Ogudo, "Development and Testing of Conversion Models from 60-minute to 1-minute Rainfall Distribution over Gqeberha, South Africa for Millimeter Wave Applications," in *8th URSI-NG Annual Conference (URSI-NG 2024)*, *Advances in Physics Research*, 2025, vol. 12: Atlantis Press-Springer Nature, pp. 245-252, doi: 10.2991/978-94-6463-644-4_24.

[20] A. Tripathi, S. Gupta, A. Mandloi, and G. G. Soni, "Optically assisted mm-wave-based multi-Gbps RoFSO transmission link under channel fading models," *Journal of Modern Optics*, vol. 69, no. 8, pp. 419-426, 2022.

[21] G. G. Soni, A. Tripathi, M. Shroti, and K. Agarwal, "Experimental study of rain affected optical wireless link to investigate regression parameters for tropical Indian monsoon," *Optical & Quantum Electronics*, Article vol. 55, no. 4, pp. 1-10, 2023. 10.1007/s11082-023-04677-0

[22] P. Tattelman and K. G. Scharr, "A model for estimating one-minute rainfall rates," *Journal of Climate and Applied Meteorology*, vol. 22, no. 9, pp. 1575-1580, 1983.

[23] J. S. Mandeep and S. I. S. Hassan, "Performances of existing rain rate models in equatorial region," *Journal of Geophysical Research: Atmospheres*, vol. 113, no. D11, 2008.

[24] A. D. Pinto-Mangones *et al.*, "Evaluation of 1-minute integration time rain rate statistics in Ecuador for radio propagation applications," *IEEE Antennas and Wireless Propagation Letters*, vol. 21, no. 7, pp. 1298-1302, 2022.

[25] "South African Weather Service." https://www.weathersa.co.za/ (accessed February 2025.

[26] P. O. Akuon and T. Afullo, "Rain cell sizing for the design of high capacity radio link systems in South Africa," *Progress In Electromagnetics Research B*, vol. 35, pp. 263-285, 2011. https://doi.org/10.2528/PIERB11083002

[27] P. A. Owolawi, "Derivation of one-minute rain rate from five-minute equivalent for the calculation of rain attenuation in South Africa," *PIERS Online*, vol. 7, no. 6, pp. 524-535, 2011.

[28] J. S. Ojo and P. A. Owolawi, "Development of one-minute rain-rate and rain-attenuation contour maps for satellite propagation system planning in a subtropical country: South Africa," *Advances in Space Research*, vol. 54, no. 8, pp. 1487-1501, 2014. https://doi.org/10.1016/j.asr.2014.06.028

[29] N. Kroese, P. Visser, A. Nhlapo, D. Terblanche, and L. Banitz, "Daily Rainfall mapping over South Africa (DARAM): Infrastructure and capacity building," in "Water Research Commission Report," 1426/1/06, 2006.

[30] R. Burger, H. Havenga, F. Hiscutt, M. Belelie, N. Ayob, and P. Kucera, "Quantifying rainfall using rain gauges, radar and satellite-real-time technologies to facilitate capacity building," in "Water Research Commission Report," 2751/1/20, 2020.

[31] ITU Radiowave Propagation Series, "Characteristics of precipitation for propagation modelling," *ITU-R Recommendation*, pp. 837-7, 2017.

[32] ITU-R Recommendation P.837-7, "Characteristics of precipitation for propagation modelling," *International Telecommunication Union, Geneva, Switzerland*, 2017.

[33] L. D. Emiliani, L. Luini, and C. Capsoni, "Extension of ITU-R method for conversion of rain rate statistics from various integration times to one minute," *Electronics Letters*, vol. 44, no. 8, pp. 557-558, 2008.

[34] ITU-R Recommendation P.839-2, "Rain height model for prediction methods," *International Telecommunication Union, Geneva, Switzerland*, 1999.

© 2025 by the authors; licensee Learning Gate

[35] ITU-R Recommendation P.839-4, "Rain height model for prediction methods," *International Telecommunication Union, Geneva, Switzerland*, 2013.
[36] ITU-R Recommendation P.618-13, "Propagation data and prediction methods required for the design of Earth-space telecommunication systems," *International Telecommunication Union, Geneva, Switzerland*, 2017.
[37] ITU-R Recommendation P.838-3, "Specific attenuation model for rain for use in prediction methods," *International Telecommunication Union, Geneva, Switzerland*, 2005.

Edelweiss Applied Science and Technology
ISSN: 2576-8484
Vol. 9, No. 8: 989-1001, 2025
DOI: 10.55214/2576-8484.v9i8.9523
© 2025 by the authors; licensee Learning Gate